

Modelling of tension-stiffening in bending RC elements based on equivalent stiffness of the rebar

Lluís Torres^{*1}, Cristina Barris^{1a}, Gintaris Kaklauskas^{2b} and Viktor Gribniak^{3c}

¹*Analysis and Advanced Materials for Structural Design (AMADE), Polytechnic School, University of Girona, Campus Montilivi s/n, 17071 Girona, Spain*

²*Department of Bridges and Special Structures, Vilnius Gediminas Technical University (VGTU), Sauletekio av. 11, 10223 Vilnius, Lithuania*

³*Civil Engineering Research Centre, VGTU, Sauletekio av. 11, 10223 Vilnius, Lithuania*

(Received November 6, 2013, Revised October 27, 2014, Accepted November 27, 2014)

Abstract. The contribution of tensioned concrete between cracks (tension-stiffening) cannot be ignored when analysing deformation of reinforced concrete elements. The tension-stiffening effect is crucial when it comes to adequately estimating the load-deformation response of steel reinforced concrete and the more recently appeared fibre reinforced polymer (FRP) reinforced concrete. This paper presents a unified methodology for numerical modelling of the tension-stiffening effect in steel as well as FRP reinforced flexural members using the concept of equivalent deformation modulus and the smeared crack approach to obtain a modified stress-strain relation of the reinforcement. A closed-form solution for the equivalent secant modulus of deformation of the tensioned reinforcement is proposed for rectangular sections taking the Eurocode 2 curvature prediction technique as the reference. Using equations based on general principles of structural mechanics, the main influencing parameters are obtained. It is found that the ratio between the equivalent stiffness and the initial stiffness basically depends on the product of the modular ratio and reinforcement ratio ($n\rho$), the effective-to-total depth ratio (d/h), and the level of loading. The proposed methodology is adequate for numerical modelling of tension-stiffening for different FRP and steel reinforcement, under both service and ultimate conditions. Comparison of the predicted and experimental data obtained by the authors indicates that the proposed methodology is capable to adequately model the tension-stiffening effect in beams reinforced with FRP or steel bars within wide range of loading.

Keywords: reinforced concrete; tension-stiffening; constitutive modelling; fibre reinforced polymer reinforcement; steel reinforcement; serviceability; numerical modelling

1. Introduction

The wider use of innovative construction materials with higher strengths for reinforcement and concrete has led to longer spans and smaller depths; consequently, Serviceability Limit State

*Corresponding author, Professor, E-mail: Lluís.Torres@udg.edu

^aLecturer, E-mail: Cristina.Barris@udg.edu

^bProfessor, E-mail: Gintaris.Kaklauskas@vgtu.lt

^cSenior Researcher, E-mail: Viktor.Gribniak@vgtu.lt

(crack width and deformations) has often become the governing criterion in the design of structural elements. This phenomenon is even more accentuated when fibre reinforced polymer (FRP) is used as internal reinforcement. With their high tensile strength, their lower modulus of elasticity compared with steel most of the times leads to a design governed by limitation of deformations.

Along with the traditional design codes, numerical methods are widely used in the design of concrete structures, so adequate modelling of material behaviour is of major importance. Previous research has shown that concrete between cracks contributes to the stiffness of the element due to interaction between the reinforcement and the concrete (usually referred to the tension-stiffening effect), and has a significant influence on the deformation analysis of reinforced concrete (RC) elements (Gilbert and Warner 1978, Floegl and Mang 1982, Gupta and Maestrini 1990, Russo and Romano 1992, Aiello and Ombres 2000, Torres *et al.* 2004, Kaklauskas 2004, Bischoff 2005, Bischoff 2007a, Gilbert 2007, Dede and Ayvaz 2009, Sarkar *et al.* 2009, Wu and Gilbert 2009, Kaklauskas *et al.* 2011a).

Different approaches have been proposed to describe tension-stiffening. Bond stress transfer models (Floegl and Mang 1982, Gupta and Maestrini 1990, Wu *et al.* 1991, Russo and Romano 1992, Choi and Cheung 1996, Aiello and Ombres 2000), in which, bond stresses between reinforcement and concrete in a cracked member are introduced using a bond stress-slip law. Due to its greater complexity and difficulty to determine some of the required parameters, these models have usually been limited to specific cases and not widely used for structures with many members. Equivalent flexural stiffness models, like the well-known Branson's equation (Bischoff 2007b), which is based on an equivalent moment of inertia, calculated by interpolating between the moments of inertia of uncracked and fully cracked sections. Average stress-strain models (CEN 2004, fib 2010), where a mean strain between the fully-cracked and uncracked states is assumed. Constitutive material models that are based on the constitutive equations specified for tensile concrete (Scanlon and Murray 1974, Lin and Scordelis 1975, Gilbert and Warner 1978, Prakhya and Morley 1990, Massicote *et al.* 1990, Kaklauskas and Ghaboussi 2001, Torres *et al.* 2004, Bischoff 2005, Stramandinoli and La Rovere 2008) or for the reinforcement (Murashev *et al.* 1971, Gilbert and Warner 1978, Moosecker and Grasser 1981, Gilbert 1983, Choi and Cheung 1994, Bischoff 2005) to predict stress-strain behaviour in a cracked section.

Constitutive material models based on the modification of the tensile branch of the concrete stress-strain relationship or the stress-strain law of the reinforcement are based on the smeared cracking approach. These approaches have been widely used for numerical modelling of RC structures, since they present a combination of a relative degree of simplicity with enough generality to be effectively used in numerical analysis.

Among the aforementioned works, a number of studies to select the values of the coefficients defining the constitutive laws for tensile concrete have been carried out (Scanlon and Murray 1974, Lin and Scordelis 1975, Kaklauskas and Ghaboussi 2001, Torres *et al.* 2004, Bischoff 2005), but only few studies have dealt with the constitutive equations specified for the reinforcement (Murashev *et al.* 1971, Gilbert and Warner 1978, Moosecker and Grasser 1981, Gilbert 1983, Bischoff 2005). Relatively early proposals (Murashev *et al.* 1971) were based on dividing the actual modulus of elasticity of the reinforcement by a coefficient depending on the relative level of loading (relationship between the load and the cracking load) in which a parabolic distribution of strains between cracks was assumed; Gilbert and Warner (1978) proposed a modified stepped stress-strain diagram for tension steel after cracking divided in intervals of strain with fixed different values of the equivalent secant modulus of elasticity of the reinforcement;

Gilbert (1983) proposed obtaining an equivalent modular ratio introducing an equivalent concrete area at the level of the reinforcement, which was adjusted with available test data and depended on the actual reinforcement and modular ratios; based on Murashev's approach, Bischoff (2005) proposed an equivalent secant modulus of elasticity as a function of the level of load (relationship between applied flexural moment and cracking moment) and a relationship between the moment of inertia and distance between tensile reinforcement and neutral axis depth for cracked and uncracked sections. Most of these models have been empirically adjusted using specific databases, or reinforcement ratios and concrete properties that were usual for steel reinforcement, but not for new types of concrete or for the unique characteristics of FRP bars. Additionally, the basic sectional parameters influencing the laws, and therefore affecting tension-stiffening, are not explicitly stated in the proposals. Therefore, providing guidelines to select proper values of the coefficients characterizing the diagrams based on primary sectional design data could be of major interest.

The present study aims at performing an analysis to rationally find the main parameters influencing tension-stiffening in flexural RC structures modelled through an equivalent reinforcement constitutive model and to propose a simple, but sound approach to obtain coefficients defining the law. Using general principles of structural mechanics, the modelling methodology is developed for rectangular sections taking Eurocode 2 (CEN 2004) as a reference model, in line with a number of studies that consider steel as well as FRP RC elements (Barris *et al.* 2009, Pilakoutas *et al.* 2011, Al-Sunna *et al.* 2012, Balázs *et al.* 2013). A closed-form equation is proposed to obtain the reinforcement equivalent secant stiffness as a function of the relevant sectional parameters. Comparison of the predicted deformations (curvatures) and experimental data of RC beams and specific tests carried out by the authors to measure the tension-stiffening effect (based on an average strain of the reinforcement), is used to validate applicability of the proposed methodology for modelling the tension-stiffening effect in flexural elements reinforced with FRP or steel bars.

2. Equivalent stiffness of the reinforcement to model the tension-stiffening effect

2.1 Equivalent secant stiffness of the reinforcement based on the Eurocode 2 model

The aim of the present study is to investigate the variation in an equivalent stiffness of the reinforcement that reproduces a defined moment-curvature trend, while taking into account the tension-stiffening effect. For this purpose, Eurocode 2 (CEN 2004) moment-curvature prediction model is adopted, since the suitability of its methodology for steel RC and FRP RC elements has been widely corroborated (Pecce *et al.* 2000, Bischoff 2005, Al-Sunna *et al.* 2012, Barris *et al.* 2009). According to Eurocode 2, the moment-curvature is interpolated between the fully cracked and uncracked states, as typically represented in Fig. 1.

Fig. 1 shows that the sectional secant stiffness varies from that of the uncracked to that of the fully cracked state and is represented by the slope of the secant line between a specific point and the origin. It is easily seen that the slope depends on the level of load as well as on some relationship between the uncracked and fully cracked lines slope. Therefore, when modelling the tension-stiffening effect through an equivalent stiffness of the reinforcement, it is presumable that the stiffness will be affected by the significant parameters involved in the sectional stiffness variation.

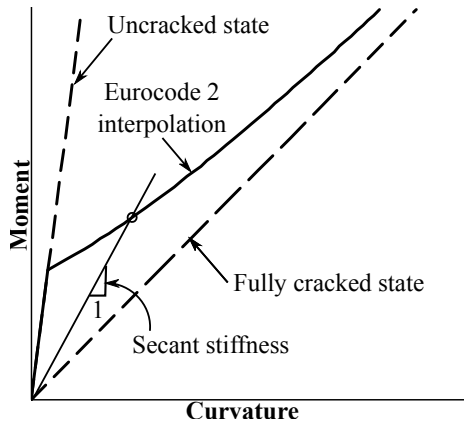


Fig. 1 Moment-curvature relationship according to Eurocode 2

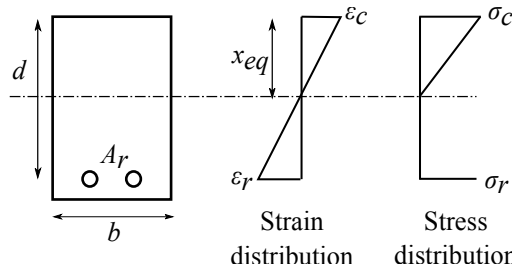


Fig. 2 Stress and strain distribution at a cross-section level

2.2 Cracked section with equivalent secant stiffness of the reinforcement

The study is limited to the serviceability range in the first part of the present paper, and hence a linear relationship for reinforcement and for compressed concrete is assumed. The analysis is performed for a cracked section ignoring concrete in tension while taking into account the equivalent stiffness of the reinforcement. The diagrams in Fig. 2 are based on these assumptions and represent strain and stress at a cross-section level for the serviceability range of loading.

Equilibrium and strain compatibility equations read

$$A_r \sigma_r = \frac{1}{2} \sigma_c b x_{eq} \tag{1}$$

$$M = A_r \sigma_r \left(d - \frac{x_{eq}}{3} \right) \tag{2}$$

$$\kappa = \frac{\epsilon_c}{x_{eq}} = \frac{\epsilon_r}{d - x_{eq}} \tag{3}$$

where σ_c and ϵ_c are the maximum stress and strain in the concrete, σ_r and ϵ_r are the stress and strain at the reinforcement, x_{eq} is the position of the equivalent neutral axis depth, b is the width of the section, A_r is the area of reinforcement, d is the effective depth, M is the flexural moment and κ is the curvature.

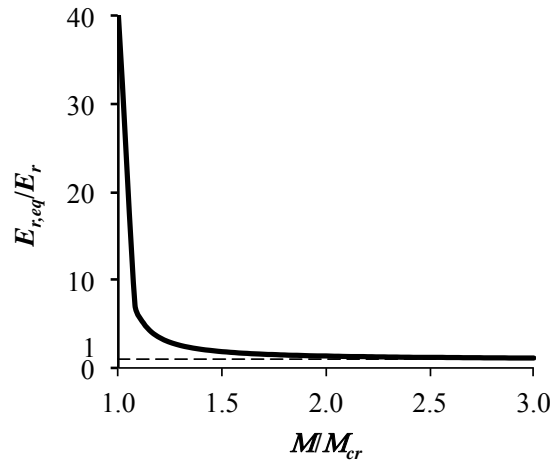


Fig. 3 Typical equivalent secant modulus of deformation relationship $E_{r,eq}/E_r$, depending on the relative load level, M/M_{cr}

Development of previous equations allows obtaining the force in the reinforcement F_r , the sectional flexural moment M , and the equivalent secant stiffness of the reinforcement $(AE)_{r,eq}$ (see Appendix A)

$$F_r = (AE)_{r,eq} \varepsilon_r = \frac{1}{2} E_c \kappa b x_{eq}^2 \quad (4)$$

$$M = \frac{1}{2} E_c \kappa b x_{eq}^2 \left(d - \frac{x_{eq}}{3} \right) \quad (5)$$

$$(AE)_{r,eq} = \frac{E_c b x_{eq}^2}{2(d - x_{eq})} \quad (6)$$

where E_c is the modulus of elasticity of concrete.

If the flexural moment M and the curvature κ are known (i.e. from the Eurocode 2 model), the equivalent neutral axis depth x_{eq} can be calculated from Eq. (5). Consequently, the equivalent stiffness can be determined from Eq. (6) at each load step by applying an inverse method (Kaklauskas *et al.* 2011b). If for the sake of simplicity the area of reinforcement is maintained as A_r , the equivalent secant modulus of deformation $E_{r,eq}$ can be obtained by rearranging Eq. (6)

$$E_{r,eq} = \frac{E_c b x_{eq}^2}{2A_r (d - x_{eq})} = \frac{E_c (x_{eq}/d)^2}{2\rho (1 - x_{eq}/d)} \quad (7)$$

where ρ is the actual reinforcement ratio and x_{eq}/d can be referred as the relative depth of the compression zone.

The variation of the equivalent secant modulus of the reinforcement $E_{r,eq}$ with the level of loading (as seen in Fig. 1) can be represented as a function of moment ratio (M/M_{cr}) where M is the applied moment and M_{cr} is the cracking moment. Fig. 3 shows a typical case of this dependency in an RC element with a section of 150×200 mm reinforced with FRP bars with a modulus of

elasticity of $E_r=80$ GPa, and a reinforcement ratio of $\rho=0.01$. The concrete compressive strength is 75 MPa and the ratio between the effective depth and the height of the beam (d/h) is 0.75. In the figure, the evolution of $E_{r,eq}/E_r$ is represented up to the point where the bending moment equals three times the cracking moment.

Fig. 3 shows that the $E_{r,eq}/E_r$ trend descends as the M/M_{cr} ratio increases, indicating that the tension-stiffening effect decreases with increasing average strain in the reinforcement. Relatively high values of $E_{r,eq}/E_r$ are observed during the first steps of cracking, which is in agreement with results from previous studies (Gilbert and Warner 1978). However, for higher load levels $E_{r,eq}/E_r$ asymptotically approaches unity, meaning that tension-stiffening disappears.

2.3 Influencing parameters

As mentioned previously, to model the tension-stiffening effect, the Eurocode 2 (CEN 2004) approach is selected as a reference. The mean curvature κ due to flexural moment M is obtained by

$$\kappa = \kappa_1(1 - \zeta) + \kappa_2\zeta \quad (8)$$

$$\zeta = 1 - \beta \left(\frac{M_{cr}}{M} \right)^2 \quad (9)$$

where κ_1 and κ_2 are the curvatures at uncracked and fully-cracked states respectively, and β is a coefficient taking account of the influence of repeated loading or the duration of sustained loading (1.0 for a single short-term loading and 0.5 for sustained or repeated loading). Using Eqs. (8)-(9), and considering short-term loading ($\beta=1$), equivalent flexural stiffness in terms of equivalent moment of inertia is given by

$$I_{eq} = \frac{I_1 I_2}{I_2 \left(\frac{M_{cr}}{M} \right)^2 + I_1 \left[1 - \left(\frac{M_{cr}}{M} \right)^2 \right]} \quad (10)$$

where I_1 and I_2 are the moments of inertia of the uncracked and fully cracked sections respectively.

On the other hand, the equivalent moment of inertia for a cracked section with equivalent secant stiffness of the reinforcement (Fig. 2) can be directly obtained from Eq. (5)

$$I_{eq} = \frac{M}{E_c \kappa} = \frac{1}{2} b x_{eq}^2 \left(d - \frac{x_{eq}}{3} \right) \quad (11)$$

By equating equivalent stiffness obtained from Eurocode 2 (Eq. (10)) and that from a cracked section with equivalent secant stiffness of the reinforcement (Eq. (11)), the following equation for the relative depth of the compression zone is obtained

$$\left(\frac{x_{eq}}{d} \right)^2 \left(1 - \frac{x_{eq}}{3d} \right) = \frac{1}{6(d/h)^3} \frac{I_2/I_1}{I_2/I_1 (M_{cr}/M)^2 + \left[1 - (M_{cr}/M)^2 \right]} \quad (12)$$

This equation indicates that (x_{eq}/d) depends on the relative effective depth of the section (d/h) and on the ratio of moments of inertia of fully cracked and uncracked section I_2/I_1 . The latter can be expressed as

$$I_2/I_1 = \frac{\frac{1}{2}bx^2(d-x/3)}{\frac{1}{12}bh^3} = \frac{6\left(\frac{x}{d}\right)^2(1-x/3d)}{\left(\frac{h}{d}\right)^3} \tag{13}$$

in which the moment I_2 has been obtained using Eq. (11) applied to a fully cracked section. The normalized neutral axis depth can be obtained from the well-known equation (fib 2010)

$$\frac{x}{d} = -n\rho + \sqrt{(n\rho)^2 + 2n\rho} \tag{14}$$

where x is the neutral axis depth of the fully cracked section, n is the modular ratio of the moduli of elasticity of the bare bar, E_r , and concrete, E_c . Consequently, I_2/I_1 in Eq. (13) and therefore in Eq. (12), depends only on $n\rho$ and d/h . The same applies to (x_{eq}/d) in Eq. (12) as well as $E_{r,eq}$ in Eq. (7) that also depends on $n\rho$ and d/h . A more detailed derivation of the above governing equations is given in Appendix A.

2.4 Parametric study

A parametric study has been performed to investigate the influence of parameter ($n\rho$) and relative effective depth (d/h) on variation of the equivalent secant modulus of deformation $E_{r,eq}$ found in Eq. (7). Covering the range of values usually found in practice, the reinforcement ratio varied from 0.005 to 0.04, the modulus of elasticity of the reinforcement ranged between 40 and 200 GPa, the concrete compressive strength varied from 25 to 70 MPa, and the d/h ratio varied from 0.75 to 0.85. In the considered cases, $n\rho$ varied from 0.01 to 0.25. Fig. 4 illustrates the effect of $n\rho$ and d/h on $E_{r,eq}/E_r$ expressed as a function of relative load level (M/M_{cr}) for a typical RC section with 150 mm width and 200 mm depth, and with a concrete strength of 25 MPa. It can be observed that the equivalent secant modulus of deformation decreases as $n\rho$ and d/h increase, which reflects the expected decrease in the tension-stiffening effect according to Eurocode 2 as these parameters increase.

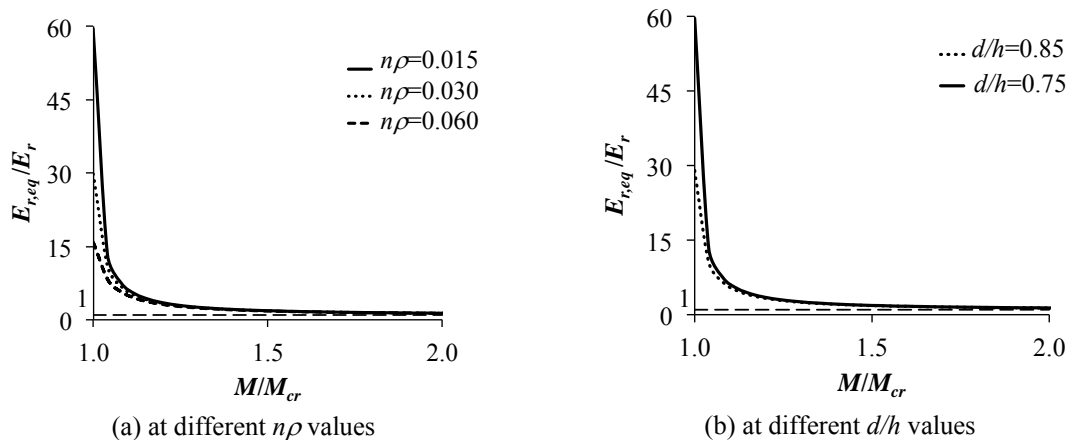


Fig. 4 Equivalent secant modulus of deformation $E_{r,eq}/E_r$ depending on the relative load level, M/M_{cr}

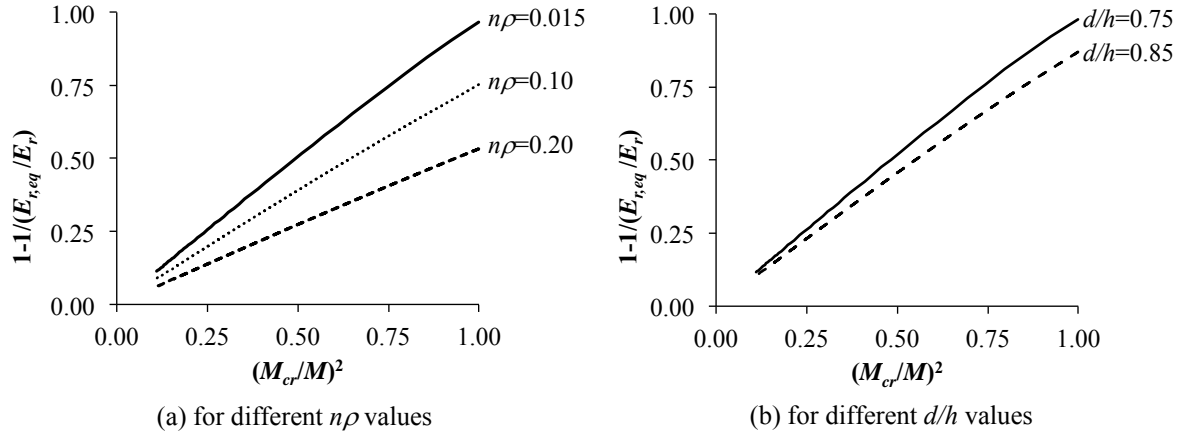


Fig. 5 Representation of normalized equivalent secant modulus of deformation

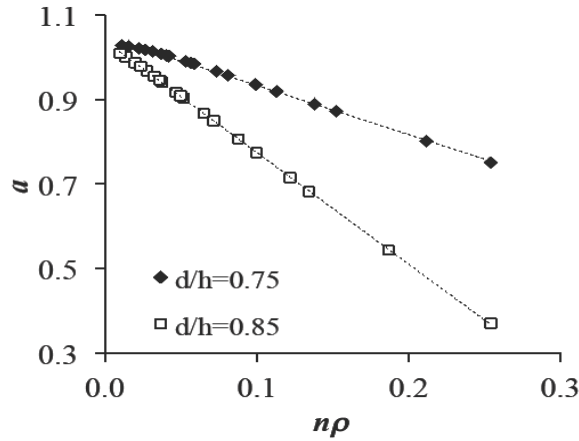


Fig. 6 Dependence of parameter a on $n\rho$ and d/h (see Eq. (13))

Different types of equations could be investigated to adjust a closed form equation for the equivalent secant modulus of deformation. Nevertheless, from the existing literature (Murashev *et al.* 1971, Bischoff 2005) it can be assumed that the relationship between the equivalent secant modulus of deformation and the load level can be expressed in the form:

$$\frac{E_{r,eq}}{E_r} = \frac{1}{1 - a\mu^2} \tag{15}$$

$$\mu = \frac{M_{cr}}{M} \tag{16}$$

where a is a dimensionless parameter. Since it has been proved that $E_{r,eq}/E_r$ depends on $n\rho$ and d/h , the effect of variation of these parameters on a are shown in Fig. 5, with a being the slope of the curves. The curves obtained are approximately straight lines with a slope that decreases as $n\rho$ (Fig. 5(a)) and d/h (Fig. 5(b)) increase.

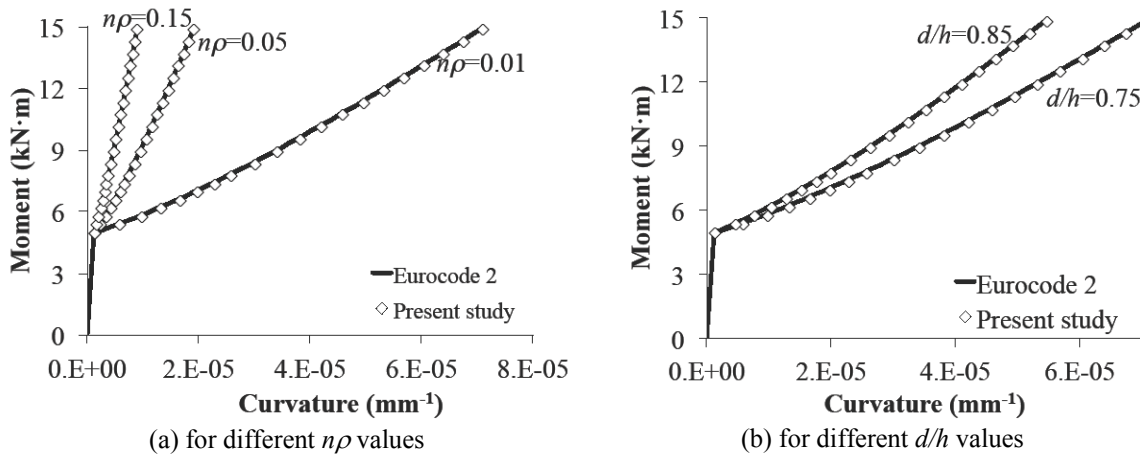


Fig. 7 Moment-curvature comparison for a typical FRP RC element

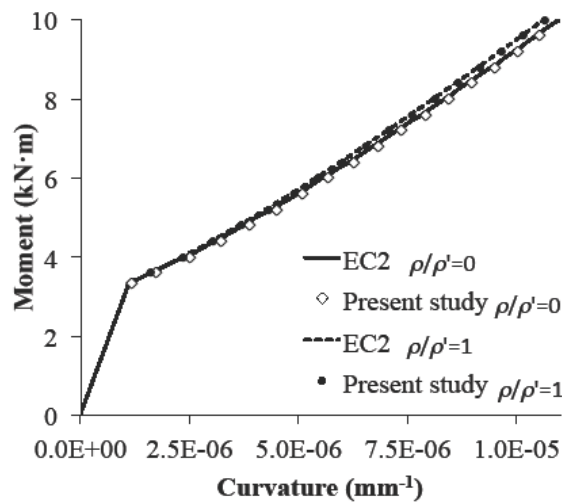


Fig. 8 Moment-curvature comparison for a typical steel RC element

Parameter a is represented as a function of $n\rho$ and d/h in Fig. 6. It can be observed that parameter a is strongly influenced by the variation of $n\rho$ with a nearly linear shape of this relationship. The influence of d/h on a by increasing the slope of the curves as d/h increases is also seen.

As can be observed from Fig. 6, the relationship between parameter a and variables $n\rho$ and d/h can be found using linear regression analysis. The obtained equation can be expressed as for practical application:

$$a = 10n\rho(1 - 1.5d/h) + 1 \quad (17)$$

Fig. 7 shows typical moment-curvature relationships for the range of values adopted in this parametric study. Good agreement between the Eurocode 2 predictions and the results using the proposed tension-stiffening model can be observed.

Eq. (17) can also be applied to a conventional steel RC section that includes compressive reinforcement. Fig. 8 represents the moment-curvature relationship for a steel RC section with 150 mm width and 200 mm depth, where $n\rho=0.06$, $d/h=0.85$, $d'/h=0.10$ and ρ'/ρ varies between 0 and 1, being ρ' the compressive reinforcement ratio. As can be seen, there are no significant differences between the curves.

A closed-form solution for the relative modulus of deformation $E_{r,eq}/E_r$ as a function of the relative load M_{cr}/M can be obtained from Eqs. (15)-(17). If a relationship for $E_{r,eq}/E_r$ based on the strain ratio $\varepsilon_r/\varepsilon_{r,cr}$ is needed, the corresponding values of the strains for M and M_{cr} can be obtained from

$$\varepsilon_r = \frac{M(d - x_{eq})}{E_c I_{eq}} \tag{18}$$

$$\varepsilon_{r,cr} = \frac{M_{cr}(d - x_1)}{E_c I_1} \tag{19}$$

where x_1 , and I_1 are, respectively, the neutral axis depth and moment of inertia of the uncracked section (as a simplification they can be substituted by the gross section parameters x_g and I_g).

2.5 Application of the methodology up to failure

The deductions made in the previous sections were performed assuming elastic behaviour of reinforcement and concrete, resulting in the procedure to model tension-stiffening suitable for the serviceability range of loads. This section illustrates applicability of the considered methodology for the entire range of loads up to failure with no loss of precision, taking into account the non-

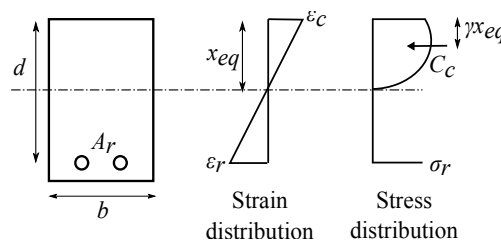


Fig. 9 Strains and stresses in Cracked Section Analysis (CSA)

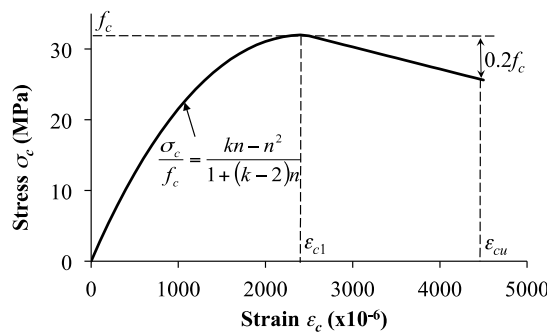


Fig. 10 Stress-strain curve of concrete in compression up to failure

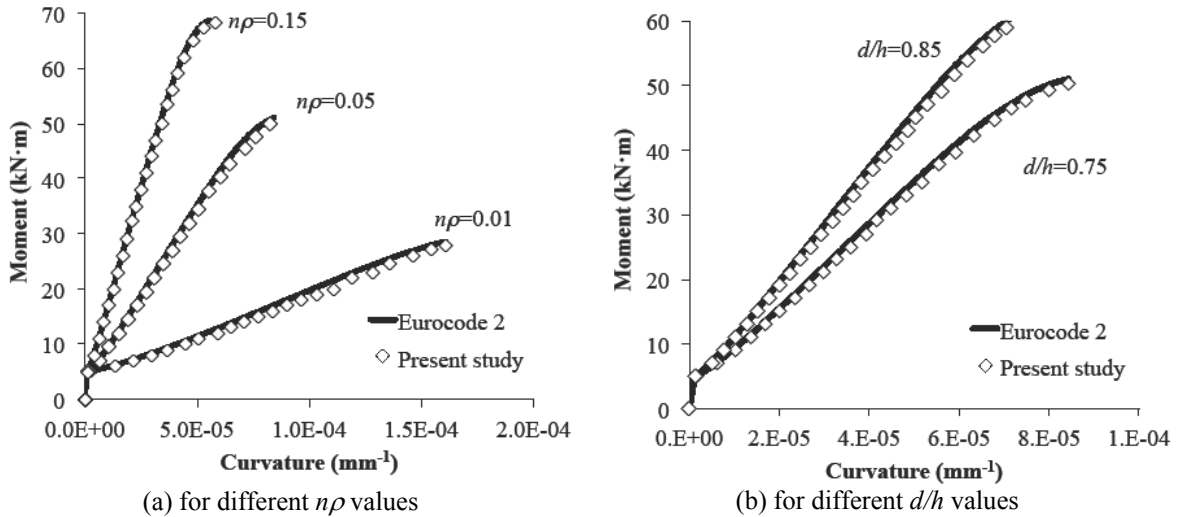


Fig. 11 Comparison of moment-curvature diagrams up to failure for a typical FRP RC element

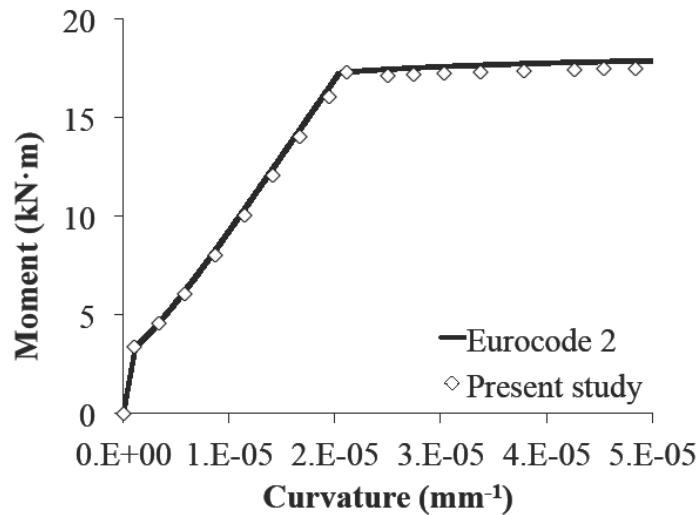


Fig. 12 Comparison of moment-curvature diagrams up to failure for a typical steel RC element

linear properties of materials. Validity of equations obtained for linear behaviour and serviceability can be justified by the reduction tendency of tension-stiffening as the load increases.

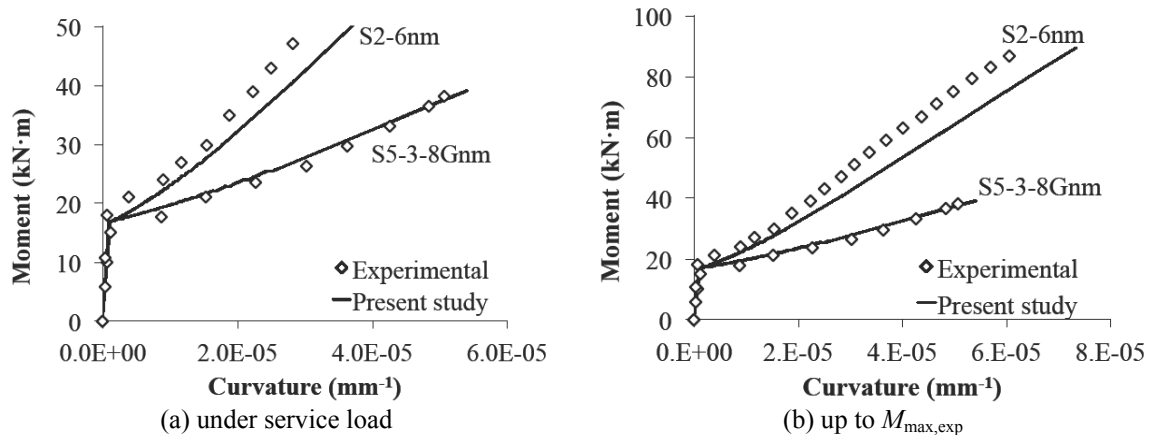
To obtain a moment-curvature response using the proposed methodology, Cracked Section Analysis (CSA) could be used (Fig. 9).

The constitutive law adopted in the present paper for concrete in compression is shown in Fig. 10 (CEN 2004).

Extending the simulation results presented in Figs. 7 and 8 at the advanced stages of loading (up to failure), resulted in moment-curvature relationships shown in Figs. 11 and 12. It can be observed that good agreement is found between the predictions made by Eurocode 2 and the proposed technique obtained both for FRP and steel reinforced members.

Table 1 Characteristics of the tested beams

Beam Designation	b (mm)	h (mm)	d/h	A_r (mm ²)	E_r (MPa)	f_c (MPa)	E_c (MPa)	f_{ct} (MPa)	$n\rho$
S2-6nm (Gribniak <i>et al.</i> 2013)	273	303	0.80	402	64433	56.0	38227	3.96	0.010
S5-3-8Gnm (Gribniak <i>et al.</i> 2013)	278	302	0.90	151	64433	45.0	36630	3.33	0.003
N-212-D1-A (Barris <i>et al.</i> 2013)	140	190	0.85	226	63437	32.1	25845	2.8	0.024
N-216-D1-B (Barris <i>et al.</i> 2013)	140	190	0.85	402	64634	32.1	25845	2.8	0.045
H-316-D1-A (Barris <i>et al.</i> 2013)	140	190	0.85	603	64634	54.5	28491	4.1	0.061
H-212-D1-S (Barris and Torres 2011)	140	190	0.85	226	200000	54.5	28491	4.1	0.070

Fig. 13 Comparison of moment-curvature diagrams of FRP RC beams with low $n\rho$ values

3. Comparison with experimental data

3.1 Moment-curvature curves

The proposed method of modelling tension-stiffening is validated using test results of six concrete beams reinforced with GFRP or steel bars coming from different experimental programs completed earlier (Barris and Torres 2011, Gribniak *et al.* 2013, Barris *et al.* 2013). The present study also includes data of newly tested beam S5-3-8Gnm. The properties of the specimens and materials are summarised in Table 1.

The analysis deals with the experimental curvatures averaged along the pure bending zone. The experimental bending moment-mean curvature response is compared with that obtained using the proposed methodology (Eqs. (13)-(15)) up to the service load and up to the maximum load applied during testing ($M_{max,exp}$) in Figs. 13-15. It should be pointed out that beams N-212-D1-A, N-216-D1-B, H-316-D1-A and H-212-D1-S were loaded up to failure.

As can be seen, there is good agreement between the experimental results and those obtained from the equation proposed for both FRP and steel RC beams.

3.2 Tension-stiffening measurement

Specimen H-316-D1-b (Barris and Torres 2011) was instrumented with strain gauges, which

were placed 22 mm apart along 250 mm on the FRP (Fig. 16), to measure the tension-stiffening effect using average strains of the FRP bar. The specimen also had a notch in the central section to

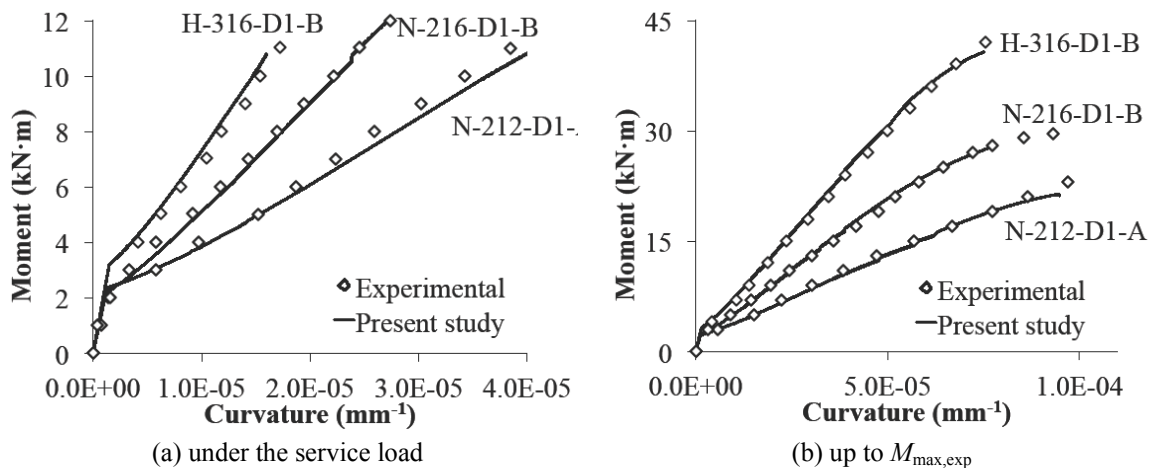


Fig. 14 Comparison of moment-curvature diagrams of FRP RC beams with high $n\rho$ values

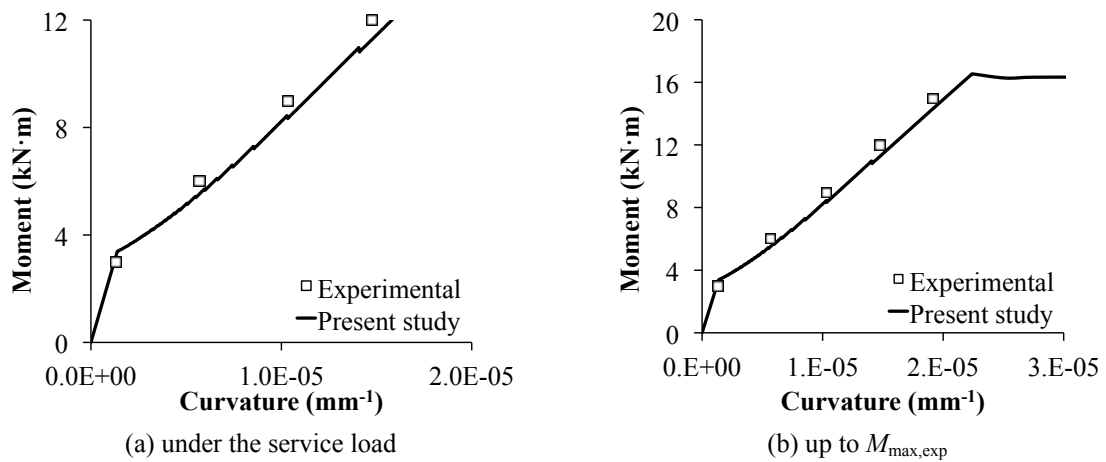


Fig. 15 Comparison of moment-curvature diagrams of a steel RC beams

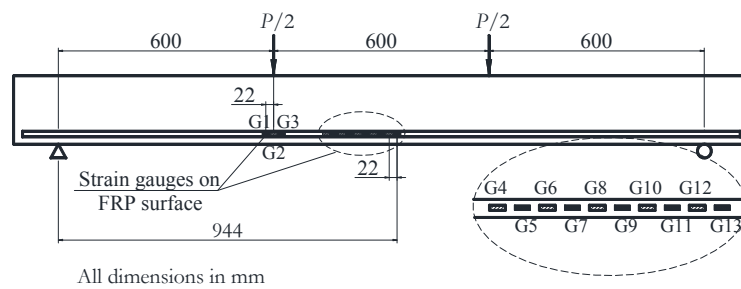


Fig. 16 Instrumentation details for beams H-316-D1-B

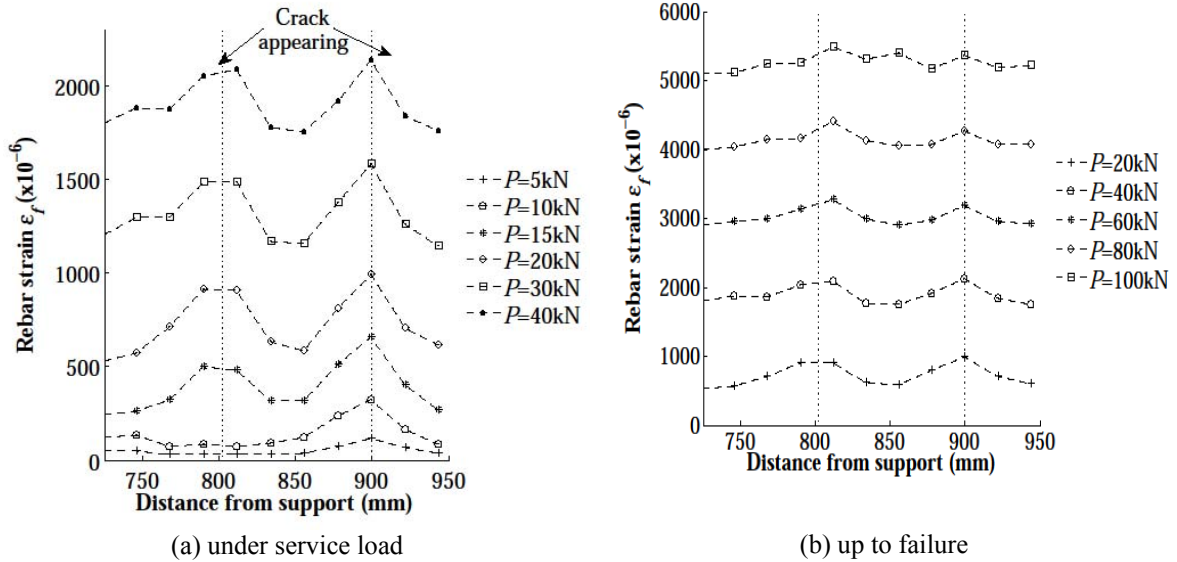


Fig. 17 Evolution of the rebar strain along part of the length of the beam

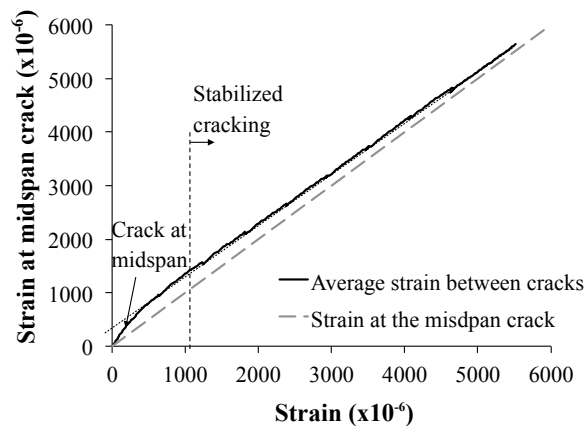


Fig. 18 Crack strain vs. average strain relationship

control the position of the crack and it was fitted with strain gauges capable of monitoring the formation and development of adjacent cracks in the central zone.

Fig. 17 shows the evolution of the rebar strains along the part of the beam that was instrumented (the dotted lines indicating the position of appearing cracks). During the crack formation phase, the strain gauges recorded the appearance of cracks with peaks in the strain curve, whereas once cracking was stabilised, the strain profile remained almost constant all along the measured length of the beam.

In Fig. 18, the rebar strain in the midspan crack (G11 in Fig. 16) is compared to the average strain at the rebar between two adjacent cracks. The strain in the crack ($\epsilon_{r,cr}$) was obtained directly from the strain profile (gauge G11), whereas the average strain ($\epsilon_{r,ave}$) was calculated by numerical integration of strain gauge readings.

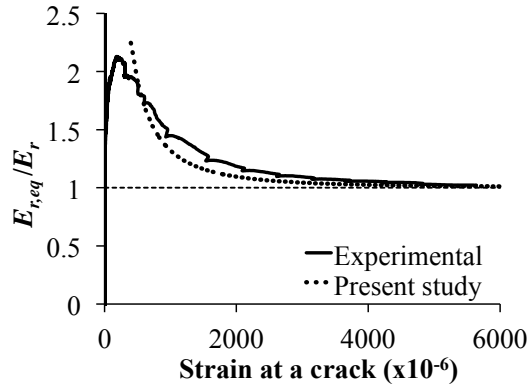


Fig. 19 Experimental and analytical values of the equivalent modulus of deformation of the reinforcement

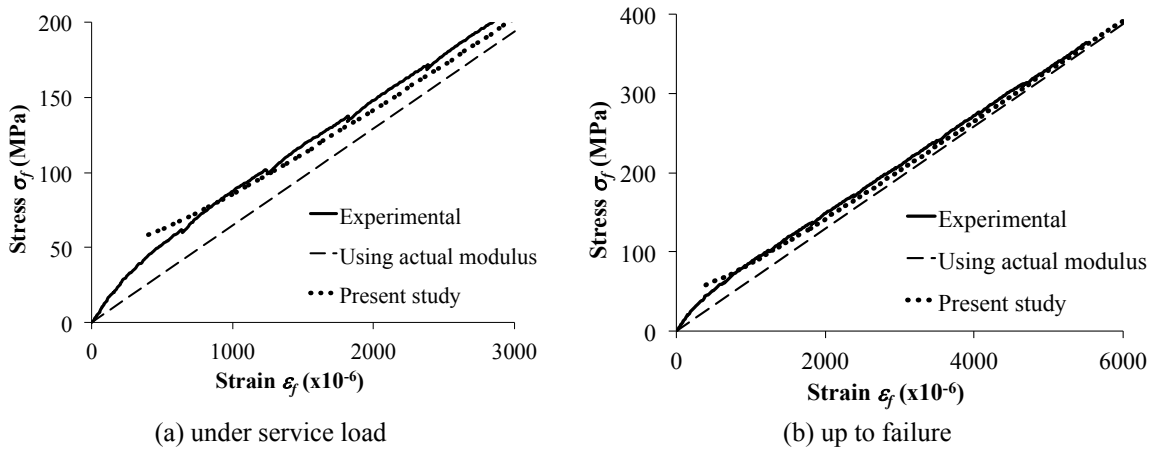


Fig. 20 Experimental and proposed values of the equivalent stress-strain curve of the reinforcement

At the crack, the tensile force is carried entirely by the reinforcement, while between cracks the force is carried by both the concrete and the rebar due to bond. Consequently, the average strain in the rebar is expected to be lower than the strain at a crack as it is observed in Fig. 18. Moreover, results show that once stabilized cracking is attained, an essentially linear relationship between the average strain and the crack strain is shown. The line representing the average strain tends to join the strain at the crack, which proves that at high load levels, tension-stiffening is almost negligible.

The effect of tension-stiffening can also be drawn as an equivalent deformation modulus of the reinforcement ($E_{r,eq}$) defined as the ratio between the stress at a flexural crack ($\sigma_{r,cr}$) and the average strain between cracks ($\epsilon_{r,ave}$) (Barris and Torres 2011). If $E_{r,eq}$ is related to the actual modulus of elasticity of the reinforcement (E_r), defined as the ratio of stress to strain at the crack ($\epsilon_{r,cr}$), the following relationship is obtained:

$$\frac{E_{r,eq}}{E_r} = \frac{\epsilon_{r,cr}}{\epsilon_{r,ave}} \quad (20)$$

Eq. (20) gives an experimental measure of the tension-stiffening effect after cracks are formed.

It is presented in Fig. 19 and compared with the ratio $E_{r,eq}/E_r$ obtained using the procedure proposed in the present study. The proposed methodology quite accurately follows the experimental trend once the first crack is formed. Obtained results show that the ratio $E_{r,eq}/E_r$ decreases and tends towards a value of 1.0 as the strain increases in the stabilized cracking phase; which means that tension-stiffening is effectively being reduced.

The tension-stiffening effect can be represented by an equivalent stress-strain curve of the reinforcement. The average stress between cracks, obtained from the strain profile, in function of the experimental strain at midspan crack is represented in Fig. 20. The equivalent modulus of deformation obtained from the present study and the bare bar modulus of elasticity are also depicted for comparison purposes. The proposed methodology satisfactorily follows the experimental trend.

4. Conclusions

The present paper introduces a methodology for numerical modelling of the tension-stiffening effect in flexural reinforced concrete elements using the concept of equivalent deformation modulus of the reinforcement. The proposed methodology has been adjusted for rectangular RC sections selecting the Eurocode 2 curvature prediction technique as reference. The main parameters influencing tension-stiffening in flexural RC structures has been rationally found. To model the tension-stiffening effect, a closed-form solution for the equivalent deformation modulus of the reinforcement has been proposed. The study draws the following specific conclusions:

- It has been established that the equivalent modulus of deformation as well as tension-stiffening is dependent on the product of the modular ratio and the reinforcement ratio ($n\rho$), the effective-to-total depth ratio (d/h), and the level of loading expressed as the ratio between the applied and the cracking moments, M_{cr}/M . The equivalent modulus decreases as $n\rho$, d/h , and M/M_{cr} increase.
- The proposed methodology accurately reproduces moment-curvature behaviour as predicted by Eurocode 2.
- Predicted results present good agreement with experimental data of both steel and FRP RC beams, including specific tests carried out to experimentally measure the tension-stiffening effect based on the average strain of the reinforcement.
- Although the constitutive equations of the equivalent deformation modulus were deduced using elastic properties of concrete, the equations are also valid for the advanced loading stages with non-linear behaviour of materials.

Acknowledgments

The authors acknowledge the support provided by the Spanish Government (Ministerio de Ciencia e Innovación), Project ref. BIA2010-20234-C03-02. The authors also gratefully acknowledge the financial support provided by the Research Council of Lithuania (Project No. MIP-083/2012) and the European Social Fund (Project No. VP1-3.1-ŠMM-08-K-01-020). Furthermore, the authors would like to thank COST Action TU 1207 “Next Generation Design Guidelines for Composites in Construction” for facilitating their collaboration.

References

- Aiello, M.A. and Ombres, L. (2000), "Cracking analysis of FRP-reinforced concrete flexural members", *Mech. Compos. Mater.*, **36**(5), 389-394.
- Al-Sunna, R.A.S., Pilakoutas, K., Hajirasouliha, I. and Guadagnini, M. (2012), "Deflection behaviour of FRP reinforced concrete beams and slabs: an experimental investigation", *Compos Part: Eng.*, **43**(5), 2125-34.
- Balázs, G.L., Bisch, P., Borosnyói, A., Burdet, O., Burns, C., Ceroni, F., Cervenka, V., Chiorino, M.A., Debernardi, P., Eckfeldt, L., El-Badry, M., Fehling, E., Foster, S.J., Ghali, A., Gribniak, V., Guiglia, M., Kaklauskas, G., Lark, R.J., Lenkei, P., Lorrain, M., Marí, A., Ozbolt, J., Pecce, M., Caldentey, A.P., Taliano, M., Tkatecic, D., Torrenti, J.M., Torres, L., Toutlemonde, F., Ueda, T., Vitek, J.L. and Vráblík, L. (2013), "Design for SLS according to fib Model Code 2010", *Struct. Concrete*, **14**(2), 99-123.
- Barris, C., Torres, L., Turon, A., Baena, M. and Catalan, A. (2009), "An experimental study of the flexural behaviour of GFRP RC beams and comparison with prediction models", *Compos. Struct.*, **91**(3), 286-295.
- Barris, C. and Torres, L. (2011), *Fibre reinforced polymer reinforced concrete beams, Serviceability behaviour: testing and analysis*, LAP LAMBERT Academic Publishing GmbH & Co.
- Barris, C., Torres, L., Comas, J. and Miás, C. (2013), "Cracking and deflections in GFRP RC beams: an experimental study", *Compos. Part: Eng.*, **55**, 580-590.
- Bischoff, P.H. (2005), "Reevaluation of deflection predictions for concrete beams reinforced with steel and fiber reinforced polymer bars", *J. Struct. Eng.*, **131**(5), 752-762.
- Bischoff, P.H. (2007a), "Rational model for calculating deflections of reinforced concrete beams and slabs", *Can. J. Civil Eng.*, **34**(8), 992-1002.
- Bischoff, P.H. (2007b), "Deflection calculation of FRP reinforced concrete beams based on modifications to the existing Branson equation", *J. Compos. Constr.*, **11**(1), 4-14.
- CEN (2004), "Eurocode 2: design of concrete structures - Part 1.1: General rules and rules for buildings (EN 1992-1-1:2004), Comité Européen de Normalisation, Brussels.
- Choi, C.K. and Cheung, S.H. (1994), "A simplified model for predicting the shear response of reinforced concrete membranes", *Thin Wall. Struct.*, **19**, 37-60.
- Choi, C.K. and Cheung, S.H. (1996), "Tension stiffening model for planar reinforced concrete members", *Comput. Struct.*, **59**(1), 179-190.
- Dede, T. and Ayzaz, Y. (2009), "Nonlinear analysis of reinforced concrete beam with/without tension stiffening effect", *Mater. Des.*, **30**(9), 3846-3851.
- fib (2010), Model Code 2010. First complete draft, Fédération International du Béton, fib Bulletin 56.
- Floegl, H. and Mang, A. (1982), "Tension stiffening concept based on bond slip", *J Struct Div*, **108**(12), 2681-2701.
- Gilbert, R.I. and Warner, R.F. (1978), "Tension stiffening in reinforced concrete slabs", *J. Compos. Constr.*, **104**(12), 1885-1900.
- Gilbert, R.I. (1983), "Deflection calculations for reinforced concrete beams", *Civil Engineering Transactions, Institution of Engineers*, 128-134.
- Gilbert, R.I. (2007), "Tension-stiffening in lightly reinforced concrete slabs", *J. Struct. Eng.*, **133**(6), 899-903.
- Gribniak, V., Kaklauskas, G., Torres, L., Daniunas, A., Timinskas, E. and Gudonis, E. (2013), "Comparative analysis of deformations and tension-stiffening in concrete beams reinforced with GFRP or steel bars and fibers", *Compos. Part: Eng.*, **50**, 158-170.
- Gupta, A.K. and Maestrini, S.R. (1990), "Tension-stiffness model for reinforced concrete bars", *J. Struct. Eng.*, **116**(3), 769-790.
- Kaklauskas, G. and Ghaboussi, J. (2001), "Stress-strain relations for cracked tensile concrete from RC beam tests", *J Struct. Eng.*, **127**(1), 64-73.
- Kaklauskas, G. (2004), "Flexural layered deformational model of reinforced concrete members", *Mag. Concrete Res.*, **56**(10), 575-584.

- Kaklauskas, G., Gribniak, V. and Girdzius, R. (2011a), "Average stress-average strain tension-stiffening relationships based on provisions of design codes", *J Zhejiang University: Science A*, **12**(10), 731-736.
- Kaklauskas, G., Gribniak, V., Salys, D., Sokolov, A. and Meskenas, A. (2011b), "Tension-stiffening model attributed to tensile reinforcement for concrete flexural members", *Proc. Eng.*, **14**, 1433-1438.
- Lin, C.S. and Scordelis, A.C. (1975), "Non linear analysis of RC shells of general form", *J. Struct. Div.*, **101**(3), 523-538.
- Massicote, B., Elwi, A.E. and MacGregor, J.G. (1990), "Tension-stiffening model for planar reinforced concrete members", *J. Struct. Eng.*, **106**(11), 3039-3058.
- Moosecker, E. and Grasser, W. (1981), "Evaluation of tension stiffening effects in reinforced concrete linear members", *Proc. Adv. Mech. Reinf. Concrete*, IABSE, 541-550.
- Murashev, V.N., Sigalov, V.I. and Baikov, E.E. (1971), *Design of reinforced concrete structures*, Zhelezobetonnye konstruksii, MIR Publishers, Moscow.
- Pilakoutas, K., Guadagnini, M., Neocleous, K. and Matthys, S. (2011) "Design guidelines for FRP reinforced concrete structures" *Proc. Inst. Civil Eng. Struct. Build.*, **4**, 255-263.
- Prakhya, G.K.V. and Morley, C.T. (1990), "Tension-stiffening and moment-curvature relations of reinforced concrete elements", *ACI Struct. J.*, **87**(5), 597-605.
- Russo, G. and Romano, F. (1992), "Cracking response of RC members subjected to uniaxial tension", *J. Struct. Eng.*, **118**(5), 1172-1190.
- Sarkar, P., Govind, M. and Menon, D. (2009), "Estimation of short-term deflection in two-way RC slab", *Struct. Eng. Mech.*, **31**(2), 237-240.
- Scanlon, A. and Murray, D.W. (1974), "Time-dependent reinforced concrete slab deflections", *J. Struct. Div.*, **100**(9), 1911-1924.
- Stramandinoli, R.S.B. and La Rovere, H.L. (2008), "An efficient tension-stiffening model for nonlinear analysis of reinforced concrete members", *Eng. Struct.*, **30**(7), 2069-2080.
- Torres, L., López-Almansa, F. and Bozzo, L.M. (2004), "Tension-stiffening model for cracked flexural concrete members", *J. Struct. Eng.*, **130**(8), 1242-1251.
- Wu, Z., Yoshikawa, H. and Tanabe, T. (1991), "Tension stiffness model for cracked reinforced concrete", *J. Struct. Eng.*, **117**(3), 715-732.
- Wu, H.Q. and Gilbert, R.I. (2009), "Modelling short-term tension stiffening in reinforced concrete prisms using a continuum based finite element model", *Eng. Struct.*, **31**(10), 2380-2391.

Appendix A. Equivalent secant stiffness and Eurocode 2 equations.

According to Fig. 2, equilibrium and strain compatibility equations for a cracked section read

$$F_r = A_r \sigma_r = \frac{1}{2} \sigma_c b x_{eq} \quad (\text{A1})$$

$$M = A_r \sigma_r \left(d - \frac{x_{eq}}{3} \right) \quad (\text{A2})$$

$$\kappa = \frac{\varepsilon_c}{x_{eq}} = \frac{\varepsilon_r}{d - x_{eq}} \quad (\text{A3})$$

where σ_c and ε_c are the maximum stress and strain in the concrete, σ_r and ε_r are the stress and strain at the reinforcement, x_{eq} is the position of the neutral axis depth, b is the width of the section, A_r is the area of reinforcement, d is the effective depth, F_r is the force in the reinforcement, M is the flexural moment and κ is the curvature.

Taking into account that the concrete maximum stress is

$$\sigma_c = E_c \varepsilon_c = E_c \kappa x_{eq} \quad (\text{A4})$$

substituting Eq. (A4) into (A1), and (A1) into (A2) the sectional flexural moment and the force in the reinforcement read

$$F_r = \frac{1}{2} E_c \kappa b x_{eq}^2 \quad (\text{A5})$$

$$M = \frac{1}{2} E_c \kappa x_{eq}^2 \left(d - \frac{x_{eq}}{3} \right) \quad (\text{A6})$$

being E_c the modulus of elasticity of concrete.

If the concept of equivalent secant stiffness of the reinforcement $(AE)_{r,eq}$ is introduced, the force in the reinforcement can be expressed as

$$F_r = (AE)_{r,eq} \varepsilon_r \quad (\text{A7})$$

Substitution of Eq. (A3) into (A7) gives

$$F_r = (AE)_{r,eq} \kappa (d - x_{eq}) \quad (\text{A8})$$

and equating (A8) and (A5) allows obtaining equivalent secant stiffness of the reinforcement as

$$(AE)_{r,eq} = \frac{E_c b (x_{eq}/d)^2}{2(1 - x_{eq}/d)} \quad (\text{A9})$$

where x_{eq}/d can be referred as the relative depth of the compression zone.

For a cracked member the mean curvature κ due to bending moment M , taking into account the tension-stiffening effect, can be calculated using the Eurocode 2 approach by

$$\kappa = \kappa_1(1 - \zeta) + \kappa_2\zeta \quad (\text{A10})$$

$$\zeta = 1 - \beta \left(\frac{M_{cr}}{M} \right)^2 \quad (\text{A11})$$

where κ_1 and κ_2 are the curvatures at uncracked and fully-cracked states respectively, M_{cr} is the cracking moment, and β is the coefficient taking account of the duration of the loading (1.0 for a single short-term loading and 0.5 for sustained or repeated loading).

From Eqs. (A10)-(A11), considering short-term loading ($\beta=1$), an equivalent flexural stiffness can be obtained in terms of equivalent moment of inertia given by

$$I_{eq} = \frac{I_1 I_2}{I_2 \left(\frac{M_{cr}}{M} \right)^2 + I_1 \left[1 - \left(\frac{M_{cr}}{M} \right)^2 \right]} \quad (\text{A12})$$

where I_1 and I_2 are the moments of inertia of the uncracked and fully cracked sections respectively.

An equivalent moment of inertia for the cracked section in Fig. , in which the stiffness of the reinforcement can vary, is directly obtained from Eq. (A6)

$$I_{eq} = \frac{M}{E_c \kappa} = \frac{1}{2} b x_{eq}^2 \left(d - \frac{x_{eq}}{3} \right) \quad (\text{A13})$$

Equating Eq. (A13), based on an equivalent stiffness of the rebar, and Eq. (A12), which derives from the reference model (Eurocode 2) gives

$$\frac{1}{2} b x_{eq}^2 \left(d - \frac{x_{eq}}{3} \right) = \frac{I_1 I_2}{I_2 \left(\frac{M_{cr}}{M} \right)^2 + I_1 \left[1 - \left(\frac{M_{cr}}{M} \right)^2 \right]} \quad (\text{A14})$$

Dividing each member of Eq. (A14) by $I_1 \approx I_g = \frac{1}{12} b h^3$, being I_g the gross moment of inertia

$$\frac{1}{2} b x_{eq}^2 \left(d - \frac{x_{eq}}{3} \right) \frac{1}{1/12 b h^3} = \frac{I_1 I_2}{I_2 \left(\frac{M_{cr}}{M} \right)^2 + I_1 \left[1 - \left(\frac{M_{cr}}{M} \right)^2 \right]} I_1 \quad (\text{A15})$$

and rearranging terms, the following equation is obtained for the relative depth of the compression zone

$$\left(\frac{x_{eq}}{d} \right)^2 \left(1 - \frac{x_{eq}}{3d} \right) = \frac{1}{6(d/h)^3} \frac{I_2/I_1}{I_2/I_1 (M_{cr}/M)^2 + \left[1 - (M_{cr}/M)^2 \right]} \quad (\text{A16})$$